SPACE WEATHER, VOL. 3, S10003, doi:10.1029/2004SW000118, 2005

Modeling the radiation belt electrons with radial diffusion driven by the solar wind

A. B. Barker[1] and X. Li

Laboratory for Atmospheric and Space Physics and Department of Aerospace Engineering Sciences, University of Colorado, Boulder, Colorado, USA

R. S. Selesnick

The Aerospace Corporation, Los Angeles, California, USA

Received 22 September 2004; revised 25 April 2005; accepted 15 July 2005; published 13 October 2005.

[1] On the basis of the correlation between the solar wind and radiation belt electron fluxes, we develop a model to simulate the MeV electron phase space density variations from $L = 3$ to $L = 8$ by extending the Li et al. (2001) radial diffusion model for geosynchronous electrons. We add L dependence to the Li et al. model and allow for comparison with measurements at more than one L shell while retaining a similar form of their diffusion coefficient. The extended model achieves a prediction efficiency (PE) of 0.61 at $L = 4$ and 0.52 at $L = 6$ when the phase space density is converted to differential flux and compared with orbit-averaged Polar 2 MeV measurements at $L = 4$ and daily averaged LANL 0.7–1.8 MeV geosynchronous measurements for the year 1998. These results indicate that radial diffusion plays a strong role in the enhancement of radiation belt electrons yet leaves a significant portion of the variance unaccounted for. We have also tuned parameters to model the electron fluxes during four individual geomagnetic storms during 1998 and found that the parameter values must differ from those of the long term and from each other to achieve the best PE. This suggests that the different solar wind drivers have varying degrees of influence on the MeV electron variations during different magnetic storms. This model can be used to forecast the MeV electron variations inside geosynchronous orbit with a reasonably good PE on the basis of real-time solar wind measurements only.

Citation: Barker, A. B., X. Li, and R. S. Selesnick (2005), Modeling the radiation belt electrons with radial diffusion driven by the solar wind, *Space Weather*, *3*, S10003, doi:10.1029/2004SW000118.

1. Introduction

[2] The MeV electrons in the outer radiation belt have been objects of study for scientists ever since their discovery at the beginning of the space age. Recently, these high-energy electrons have become increasingly important because of the potential radiation damage to spacecraft [*Gussenhoven et al.*, 1987; *Baker et al.*, 1996; *Fennell et al.*, 2001] and astronauts. To mitigate these hazards, a real-time prediction model could give operators time to put their spacecraft in to a safer, low-power mode, and astronauts could retreat to a well-shielded area. Currently, it is not well understood how the electrons are accelerated to relativistic energies, and this lack of understanding impedes their prediction to a desirable accuracy (e.g., >80%). By better understanding the electron acceleration, we should be better able to predict them.

[3] The major processes believed to play a role in the electron energization are: radial diffusion [*Fälthammar*, 1965; *Schulz and Lanzerotti*, 1974; *Selesnick et al.*, 1997; *Brautigam and Albert*, 2000; *Hilmer et al.*, 2000], rapid transport due to interplanetary shock-induced electric fields [*Blake et al.*, 1992; *Li et al.*, 1993], and local heating via wave-particle interactions [*Temerin et al.*, 1994; *Horne and Thorne*, 1998; *Summers et al.*, 1998; *Meredith et al.*, 2001, 2002; *Albert*, 2002]. These mechanisms are not mutually exclusive, and most likely each of them operates during certain levels of geomagnetic activity and in certain regions of the magnetosphere.

[4] In this study, we focus on the contribution of radial diffusion to accelerating relativistic electrons. Radial diffusion, like all diffusion processes, requires a gradient in at least one quantity and multiple perturbations of the particles. In the case of radial diffusion, there is a radial gradient in phase space density, and the perturbations are electric and magnetic field fluctuations with frequencies near the electrons' drift frequencies. The field perturbations accelerate the electrons through resonant interaction with their azimuthal drift motion [e.g., *Schulz and Lanzerotti*, 1974; *Elkington et al.*, 2003]. The rate of change in phase space density due to diffusion and

[1]Deceased 28 May 2005.

Copyright 2005 by the American Geophysical Union

losses, such as pitch angle diffusion, is described by *Schulz and Lanzerotti* [1974]

$$\frac{\partial f}{\partial t} = L^2 \frac{\partial}{\partial L}\left(\frac{D_{LL}}{L^2}\frac{\partial f}{\partial L}\right) - \frac{f}{\tau} \quad (1)$$

where f is phase space density, τ is the electron lifetime, and D_{LL} is the diffusion coefficient which determines the rate of diffusion. The quantity L represents radial distance in the equatorial plane of a dipole field and is given by $L = 2\pi M/(\Phi R_E)$ where M is the Earth's magnetic dipole moment, Φ is the third adiabatic invariant, and R_E is the radius of the Earth [*Roederer*, 1970]. While phase space density is the preferred quantity in theoretical work, flux is the quantity measured by satellites. To convert between the two, the following relation is used:

$$F = j/p^2 \quad (2)$$

where j is differential flux and p is the relativistic momentum.

[5] The radiation belt electron behavior is of particular interest during periods of high solar wind speed, often associated with increased geomagnetic activity, because electron flux is known to enhance during these periods [e.g., *Paulikas and Blake*, 1979]. Also correlated with solar wind speed is ULF (ultralow frequency) wave power [*Vennerstrom*, 1999]. ULF waves, with frequencies around 1 MHz, overlap the frequency range of the drift motion of MeV electrons, and are believed to be associated with radial diffusion. The increased ULF wave power should correspond to an increase in D_{LL}, resulting in faster diffusion during magnetic storms.

[6] The goal of this work is to first develop a radial diffusion model which uses solar wind measurements as input to predict the relativistic electron fluxes at multiple L shells. This model can provide satellite operators with advance warning of about 1–2 days at geosynchronous orbit and 3–4 days at $L = 4$ before electron enhancements, as well as help us to determine how well radial diffusion can describe the radiation belt electron flux variations. We also use the model to understand how the drivers of radial diffusion change during different magnetic storms.

2. Previous Work

[7] There have been previous attempts to model the radiation belt electron flux using radial diffusion. A few of these studies are described below.

2.1. *Selesnick et al.* [1997]

[8] During the middle of 1996, there was an approximately 3 month period in which the high-energy electron flux was characterized by inward diffusion and decay. *Selesnick et al.* [1997] used radial diffusion with loss, but no sources to model the electrons in the L range of 3 to 6. They solved equation (1) by assuming the diffusion coefficient and electron lifetime to be given by $D_{LL} = D_0(L/4)^n$ and $\tau = \tau_0(4/L)^m$, respectively. The parameters values were found using a least squares fit to Polar electron flux measurements converted to phase space density. Those values are $D_0 = (2.1 \pm 0.2) \times 10^{-3}$ d^{-1}, $n = 11.7 \pm 1.3$, $\tau_0^{-1} = (5.0 \pm 0.1) \times 10^{-2}$ d^{-1}, and $m = 7.6 \pm 0.4$. This model was able to reproduce the phase space density for electrons with a first adiabatic invariant of 6000 MeV/G, but the electrons with $\mu = 1000$ MeV/G required a source at $L > 6$.

2.2. *Brautigam and Albert* [2000]

[9] *Brautigam and Albert* [2000] used radial diffusion to model the electron fluxes during the 9 October 1990 magnetic storm over the ranges of $L = 3-6$ and $\mu = 20-1250$ MeV/G. They solved equation (1) by making the diffusion coefficient a function of Kp as well as L. Their equations for the magnetic and electric diffusion coefficients, respectively, are

$$D_{LL}^M = 10^{(0.506Kp-9.325)}L^{10},$$

$$D_{LL}^E = \frac{1}{4}\left(\frac{cE_{\rm rms}}{B_0}\right)^2\left[\frac{T}{1+(\omega_D T/2)^2}\right]L^6,$$

with

$$E_{\rm rms} = 0.26(Kp-1) + 0.1 \text{ mV/m}$$

where ω_D is the electron drift frequency, $E_{\rm rms}$ is the root mean square of the electric field amplitude, T is the exponential decay time, B_0 is the Earth's dipole moment, and E_0 is the electron rest energy. The authors converted phase space density to flux using equation (2) and were able to fairly well reproduce CRRES data for $\mu \leq 314$ MeV/G, but found that the model did poorly compared with data for μ 700 MeV/G since the phase space density from CRRES was consistent with a local source inside $L = 4.5$.

2.3. *Li et al.* [2001]

[10] *Li et al.* [2001] modeled the MeV electron fluxes at geosynchronous orbit for the years 1995–1999. Their diffusion coefficient, D_{LL}, and average electron lifetime, τ, are given by $D_{LL} = D_0(L/6.6)^{10}$ and $\tau = \tau_0(6.6/L)^{10}$, where D_0 is made a function of solar wind parameters and $\tau_0 = 2.67$ days. The function used for D_0 is

$$D_0 = C\left(\frac{v}{v_0}\right)^{\gamma_1}\left[1+\left(\frac{v_x b_z + |v_x b_z|}{\alpha}\right)^2\right]^{\gamma_2} \times \left[\frac{(\Delta v^2/\Delta t)^2}{\beta}\right]^{\gamma_3} \quad (3)$$

where C is a constant that adjusts the diffusion rate, v is solar wind speed and v_0 is its average for the years 1995–1996, α is a tunable parameter, and β is the average of $(\Delta v^2/\Delta t)^2$ for 1995–1996. The γ parameters determine the contribution of the three terms, which represent different ways energy can be transferred into the magnetosphere.

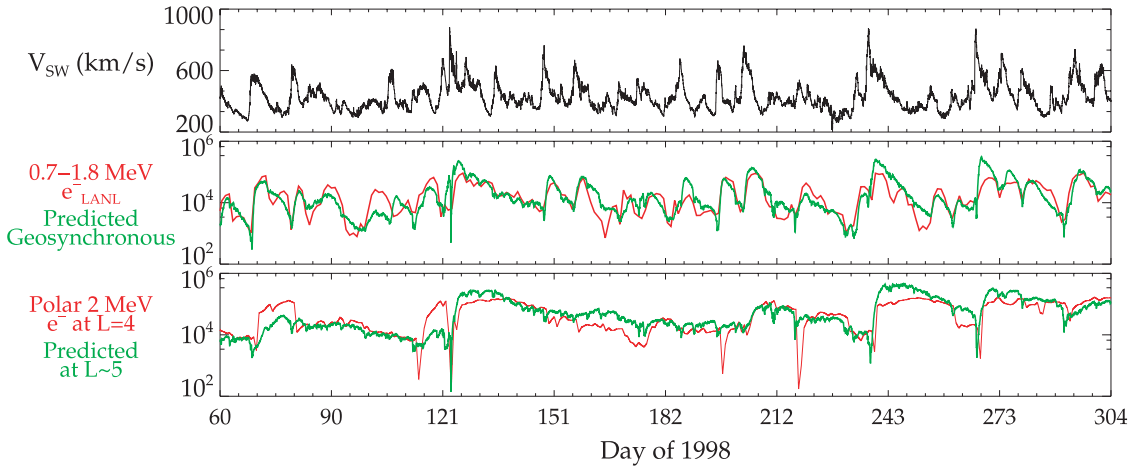

Figure 1. (top) Solar wind velocity, (middle) comparison of *Li et al.* [2001] prediction and LANL measurements at geosynchronous orbit of daily averaged differential electron flux (el cm^{-2} s^{-1} sr^{-1} MeV^{-1}), and (bottom) comparison of prediction at $L \approx 5$ and Polar electron data at $L = 4$ for a portion of 1998.

The first term is a function of solar wind speed, whose energy can be transferred through the Kelvin-Helmholtz instability. The second term is a function of the convection electric field produced by the x component of the solar wind speed, v_x, and the z component of the magnetic field, b_z; this term will be unity for northward IMF (interplanetary magnetic field), and represents the transfer due to dayside reconnection. The third term is a function of solar wind speed fluctuations, which can induce waves through direct perturbation of the magnetosphere. The phase space densities of the model's inner and outer boundaries, set at $L = 4.5$ and $L = 11$, respectively, are kept constant, with the phase space density at the outer boundary set to 10^4 times that of the inner boundary (on the basis of Wind electron measurements during the perigee passes of August and September 1996).

[11] After calculation using the diffusion equation, the phase space density is adjusted/textitad hoc to take into account the adiabatic response of the radiation belts to *Dst* and the effect of solar wind dynamic pressure. When the ring current is enhanced, the total magnetic field inside the drift orbit of a trapped particle decreases. Therefore the particle moves outward to conserve its third adiabatic invariant. The steep negative slope of the particle energy spectrum as well as a possible outward pointing phase space density gradient will cause a detector at a fixed location to observe a decrease in particle flux at a particular energy. This occurrence, known as the *Dst* effect [*Li et al.*, 1997], is implemented by adjusting f using

$$f(t+\Delta t) = f(t) \times \exp\left[\frac{Dst(t+\Delta t) - Dst(t)}{Dst_n}\right] \tag{4}$$

where Dst_n determines the magnitude of the correction. If the data were given at constant values of the three adiabatic invariants, then according to Liouville's theorem, phase space density would be conserved and the above correction would be unnecessary. Since the LANL data are taken at a constant energy and radial distance instead, electrons from different μ and L values (the dayside magnetosphere is compressed and the nightside is stretched) are measured, and the correction is required if the prediction is to compare well with the data. The dynamic pressure effect is implemented using

$$F = F \times \exp\left[-(p/p_n)^{0.6}\right] \tag{5}$$

where p is dynamic pressure and p_n determines the magnitude of the correction. The explanation for implementing the dynamic pressure effect in this way is that an increase in dynamic pressure will cause increased loss due to magnetopause shadowing.

[12] The phase space density of the model output can be converted to differential flux using equation (2). The modeled flux is compared to measured flux after multiplying the prediction by a vertical scaling factor which minimizes the mean square residual and maximizes the prediction efficiency, defined as

$$\begin{aligned} \mathrm{PE} &= 1 - \frac{\text{mean square residual}}{\text{variance of data}} \\ &= 1 - \frac{\sum_i^n (m_i - p_i)^2}{\sum_i^n (m_i - \bar{m})^2} \end{aligned} \tag{6}$$

where the residual is the difference between the data and the prediction; m_i and p_i are the measurements and model results, respectively; and $\bar{m}$ is the mean of all m_i. A prediction efficiency (PE) of zero means that the prediction is as good as saying that the value in the

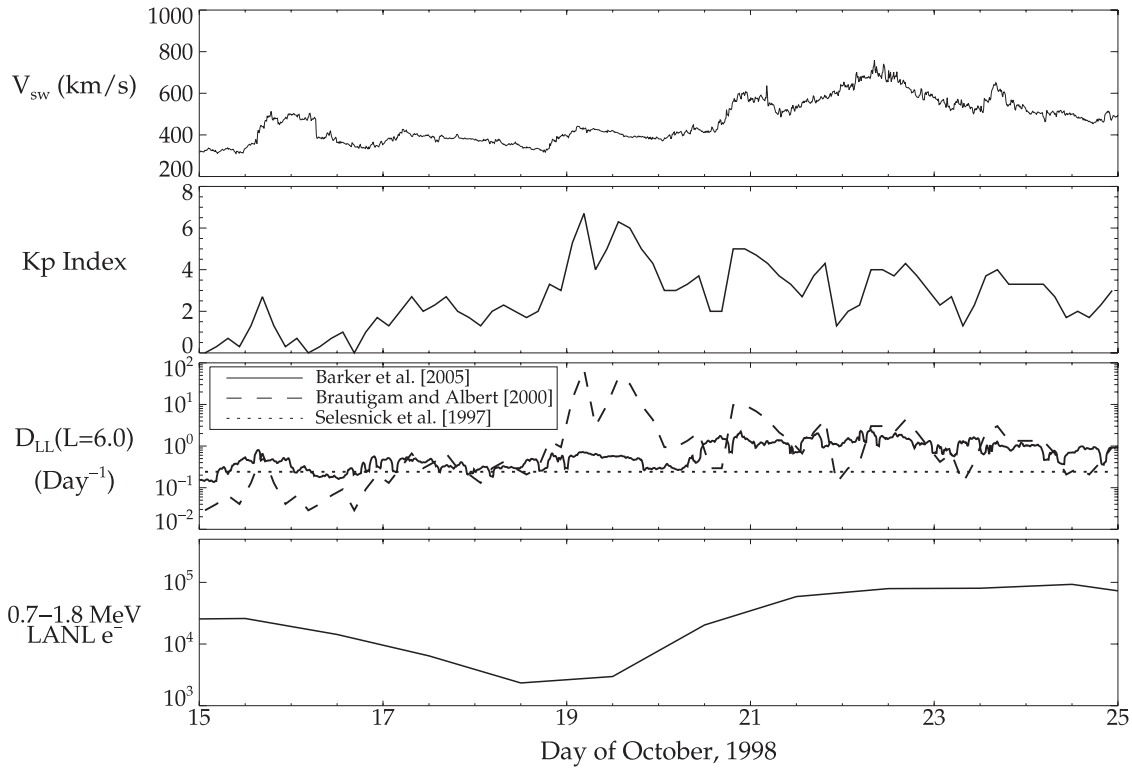

Figure 2. (top to bottom) Solar wind speed, *Kp* index, diffusion coefficients of models, and measured differential electron fluxes.

future will be the average value. A positive PE means that the prediction is better than predicting the average. The model parameters were tuned to achieve a PE of the logarithm of electron flux of 0.81 and a linear correlation (LC) of 0.90 for the years 1995–1996 on the basis of a comparison with daily averaged LANL geosynchronous 0.7–1.8 MeV electron data. Figure 1 illustrates the predictive capabilities of this model as well as the correlation of electron flux with solar wind speed. *Li et al.* [2001] were also able to reproduce some of the physical characteristics of the radiation belts and offer explanations using radial diffusion. The characteristics include the 1–2 day delay between changes in solar wind velocity and changes in electron flux, the better correlation of flux with solar wind velocity than interplanetary magnetic field direction, and the large change in electron flux for a relatively small change in solar wind speed. These results demonstrate that the correlation between solar wind conditions and relativistic electron flux at geosynchronous orbit can be well described using radial diffusion.

3. Extension of *Li et al.* [2001]

3.1. Motivation for Extension

[13] We extend the *Li et al.* [2001] model because it provides a more realistic parameterization of the diffusion coefficient than other previous work. The constant diffusion coefficient used by *Selesnick et al.* [1997] worked well for the time period they investigated, but would not be effective for more geomagnetically active periods. The D_{LL} used by *Brautigam and Albert* [2000] is time-dependent because of its dependence on *Kp*. However, since *Kp* is a result of geomagnetic activity (as are the radiation belt electron variations) rather than a cause, a diffusion coefficient parameterized by the *Kp* index cannot identify the driver of the variations. In addition, *Kp* is not as well correlated with electron flux as solar wind parameters (such as speed) are. Figure 2 demonstrates this fact.

[14] The *Li* [2004] model was designed to simulate geosynchronous electrons, which it does well. However, as shown in Figure 1, it was necessary to run the model at $L \approx 5$ in order to achieve a decent reproduction of the Polar electron flux at $L = 4$. This indicates that the modeled electrons are diffusing too slowly since by the time they have reached $L \approx 5$, they look like the measured electrons at $L = 4$. Therefore significant changes need to be made if a single model is to be used to predict MeV electron flux throughout the outer radiation belt zone.

3.2. *L* Dependence of the Diffusion Coefficient

[15] As was described above, the electrons modeled by *Li et al.* [2001] diffuse too slowly inside geosynchronous orbit. However, if the *L* dependence inside geosynchro-

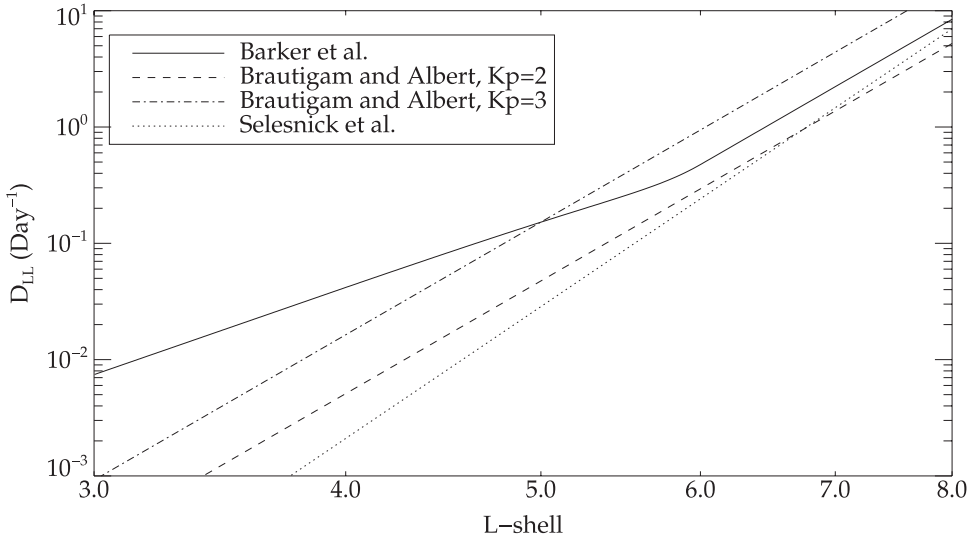

Figure 3. Diffusion coefficient versus L from several different models. Our diffusion coefficient (solid line) is averaged over all of 1998.

nous orbit is less steep, then the rate of diffusion would increase for $L < 6$, improving the prediction at $L = 4$.

[16] Theoretically, the L dependence of the diffusion coefficient should differ depending on the type of field fluctuation. If the diffusion is driven by fluctuations in the electric potential field, then the diffusion coefficient has a L^6 dependence; if driven by magnetic field fluctuations, then the dependence is L^{10} [see, e.g., *Fälthammar*, 1965; *Schulz and Lanzerotti*, 1974]. In the outer magnetosphere, the magnetic field due to the Earth's internal field is weak, and therefore the total magnetic field in that region is very susceptible to external fluctuations, such as solar wind dynamic pressure variations. However, close to the Earth, the internal magnetic field dominates, reducing the impact of external magnetic perturbations. In addition, *Rowland and Wygant* [1998] show that the electric field magnitude varies with radial distance from the Earth, and that the magnitude has been observed to increase with decreasing radial distance during periods of strong magnetic activity. We vary the exponent in D_{LL} as a power law from 10 at $L = 6$ to 6 at $L = 4$, and keep the exponent constant outside of that range. An example of what our diffusion coefficient looks like is shown in Figure 3, along with D_{LL}^M from *Brautigam and Albert* [2000] at $Kp = 2$ and 3 and D_{LL} from *Selesnick et al.* [1997]. The diffusion coefficient plotted from our model is averaged over all of 1998.

3.3. Boundary Conditions

[17] The outer boundary of the extended model is moved from $L = 11$ in the *Li et al.* model to $L = 8$ and the source at that boundary is made a function of solar wind parameters. This is done by using the form of equation (3), a general function of solar wind, but with the constant C in phase space density units rather than the inverse days of the diffusion coefficient. The source parameters were determined by maximizing the PE at $L = 6$ for all of 1998. The resulting parameter values were then used to model all time periods. When compared to Polar measurements at $L = 8$ converted to phase space density, the source phase space density is typically about an order of magnitude larger than the measurements. However, Polar was farther away from the equator at larger L, and could only measure electrons at small equatorial pitch angles. Therefore the electrons sampled are very different than those we have modeled, limiting the validity of the electron measurements in our case.

[18] The inner boundary is moved from $L = 4.5$ to $L = 3$ to allow for prediction at lower L shells. The value at the inner boundary is constant and set to always be less than the phase space density at $L = 4$, which reflects the nominal state of the radiation belts and ensures inward radial diffusion. The model results are fairly insensitive to the exact value at the inner boundary: changing the phase space density at the inner boundary by a factor of 10 up or down results in a <0.6% change in PE with all other parameters kept the same. All predictions were made using the same value at the lower boundary. That value is approximately the average of the limited Polar measurements at $L = 3$ converted to phase space density. Thus the discrepancy at the outer boundary makes the modeled phase space density gradient larger than the gradient as measured by Polar.

3.4. Other Changes

[19] The *Li et al.* [2001] implementation of the dynamic pressure effect, which was interpreted in section 2 as increased magnetopause shadowing during periods of increased dynamic pressure, should have a larger effect on the prediction at $L = 6$ than at $L = 4$ since the outer electrons are closer to the magnetopause and more likely

Table 1. Modeling Results for All Five Time Periods Investigated and Values of Parameters From Equations (1) and (3) for All Time Periods and the Source Population

	PE	LC	γ_1	γ_2	γ_3	C	p_n	Dst_n	τ, days
All of 1998									
$L = 4$	0.61	0.78	1.30	0.016	0.220	0.43	57	55	$3(6/L)^{5.3}$
$L = 6$	0.52	0.73	1.30	0.016	0.220	0.43	3	55	$3(6/L)^{5.3}$
May									
$L = 4$	0.62	0.79	0	0.085	0	0.68	6	57	$3(6/L)^{2}$
$L = 6$	0.42	0.65	0	0.085	0	0.68	2.1	57	$3(6/L)^{2}$
June									
$L = 4$	0.65	0.82	2.40	0.350	0.05	0.50	11	28	$3(6/L)^{1.15}$
$L = 6$	0.14	0.38	2.40	0.350	0.05	0.50	2.8	28	$3(6/L)^{1.15}$
September									
$L = 4$	0.59	0.77	0.04	0.003	0.006	0.61	12	68	$3(6/L)^{5.35}$
$L = 6$	0.65	0.81	0.04	0.003	0.006	0.61	3.4	68	$3(6/L)^{5.35}$
October									
$L = 4$	−0.33	0.38	0.38	0.002	0.180	0.31	40	68	$3(6/L)^{5.6}$
$L = 6$	0.67	0.84	0.38	0.002	0.180	0.31	3	68	$3(6/L)^{5.6}$
Source									
$L = 8$	—	—	2.45	0	0	3.04	—	—	—

to be lost through it. Thus we vary the parameter p_n as a function of L accordingly. For simplicity, the function is linear in L. We retain the adjustment due to the *Dst* effect from the *Li et al.* model at all L even though the Polar data is at a specified L shell. This is because the data is at a constant energy, and the flux will therefore be affected by the adiabatic response to the *Dst*. Another small modification includes setting α, the free parameter in equation (3), to be the average of $v_x b_z + |v_x b_z|$ for the years 1995–1996. This modification removes the unphysical adjustment to the $v_x b_z$ term allowing only the adjustment of the relative impact of the entire term.

[20] In the *Li et al.* [2001] model, converting from the phase space density calculated by the model to differential flux for comparison with the satellite data required only a constant factor, which was absorbed in the scaling to minimize the mean square residual. In the extended model, predictions are made at more than one L shell. Since the energies are different at the different L, the conversion factors are also different, requiring that the phase space density from the model be explicitly converted to flux before comparison with data.

[21] The phase space density of the model is converted to flux using equation (2), where the momentum is determined by the energy of the electrons as follows: The measured fluxes used to compare with model results at $L = 4$ have an energy of 2 MeV. That energy is used to find p^2 to convert to flux at $L = 4$. Assuming a dipole field, these electrons have a magnetic moment of 1220 MeV/G. An electron with the same μ value at $L = 6$ would have an energy of 0.92 MeV, which is the value used in the conversion to flux. However, the 0.7–1.8 MeV LANL energy channel used to compare with the model results at $L = 6$ has an equivalent energy of 1.1 MeV. This value was determined by calculating the single energy which gives the same flux as measured in the energy range on the basis of the average energy spectrum. The spectrum was found using an exponential fit (giving an *e*-folding energy of 0.41 MeV) to the flux measurements in the 0.7–1.8, 1.8–3.5, and 3.5–6.0 MeV LANL energy channels averaged over the year of 1998. The *e*-folding energy found above was used to adjust the 0.92 MeV modeled flux to compare with the 1.1 MeV measured flux at $L = 6$.

4. Data

[22] The solar wind data used as inputs to the model were measured by the Wind [*Acuna et al.*, 1995] and ACE [*Stone et al.*, 1998] spacecraft. To test the accuracy of the model, we compare with orbit-averaged differential electron flux measurements from the HIST instrument on the Polar satellite [*Blake et al.*, 1995; *Selesnick et al.*, 1997] at $L = 4$ and daily averaged fluxes from the Los Alamos National Laboratory (LANL) satellites at geosynchronous orbit [*Belian et al.*, 1992].

5. Results and Discussion

[23] We used the extended model to make predictions at $L = 4$ and $L = 6$ for all of 1998, and for four individual magnetic storms during that year. These L shells are of particular interest because $L = 4$ is the nominal peak of intensity for the relativistic electron flux and $L = 6$ is approximately the average L shell at geosynchronous orbit. Because of the well-known delay between solar wind speed enhancement and enhancement of the high-energy electrons [e.g., *Paulikas and Blake*, 1979], our model makes predictions of the electron flux at these two L shells days in advance. Advanced warning can be 1–2 days at geosynchronous orbit because of the lag between solar wind speed variations and MeV electron flux. The advanced warning at $L = 4$ can be as high as approximately 4 days because of the average 2-day additional delay between the peaks in flux at geosynchronous orbit and $L = 4$.

[24] To make the predictions, the following parameters can be varied: C, γ_1, γ_2, γ_3, τ, Dst_n, and p_n from equations (1), (3), (4), and (5). The parameter values were obtained by maximizing

$$\mathrm{PE}_T = \frac{1}{2}(\mathrm{PE}_4 + \mathrm{PE}_6)$$

where PE_4 and PE_6 are the PEs at $L = 4$ and 6, respectively. This method sacrifices a higher PE at a single L for the best collective PE. Our functional form for the electron lifetime is the same as that of *Selesnick et al.* [1997]: $\tau = \tau_0(6/L)^m$. The values of τ were limited to 3 days at $L = 6$ and 29 days at $L = 4$ to keep the lifetimes from being unrealistically large [*Selesnick et al.*, 1997]. However, the optimum value of m in all time periods except the October 1998 storm was such that $\tau < 29$ days at $L = 4$, though the $\tau = 3$ days at $L = 6$ consistently yielded the best PE_T. The parameter values are given in Table 1 for each of the time

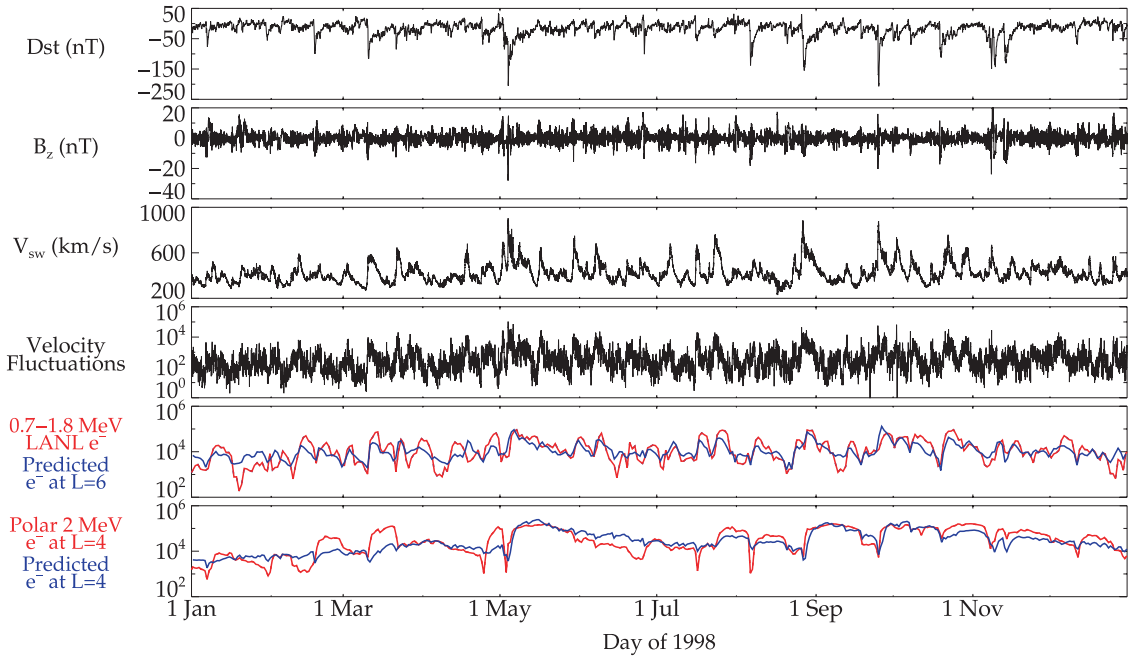

Figure 4. (top to bottom) *Dst* measurement, interplanetary magnetic field strength in the z direction, solar wind velocity, solar wind velocity fluctuations, comparison of prediction at $L = 6$ and LANL geosynchronous electron data, and comparison of prediction at $L = 4$ and Polar electron data at $L = 4$ for all of 1998.

periods investigated. Also presented in Table 1 are the PE and LC values, as well as the parameters for the source at $L = 8$.

5.1. Long-Term Prediction

[25] Figure 4 shows the results of the extended model at $L = 6$ plotted with geosynchronous electrons in the energy range 0.7–1.8 MeV, and the prediction at $L = 4$ plotted with 2 MeV electrons at $L = 4$, for all of 1998. For that time period, the model achieved a PE of 0.52 at $L = 6$ and 0.61 at $L = 4$ using the parameters listed in Table 1. Focusing on the flux measurements (red curves) in the bottom two plots, it is evident that the electron flux varies on very different timescales at the two L shells. Thus the model's ability to fairly well predict the flux at both L shells makes it very likely that radial diffusion plays a strong role in energizing the relativistic electrons in the radiation belt. However, our model is still unable to completely describe the flux variations at both L shells. This indicates that the model either does not sufficiently simulate the radial diffusion in the Earth's magnetosphere or other processes, such as wave-particle interactions, are also acting.

[26] To transport particles inward, radial diffusion requires an outward pointing phase space density gradient. Through the processes of diffusion and loss, this gradient usually exhibits extensive variability, which is demonstrated by the ratio of phase space densities at $L = 6$ and $L = 4$ shown in Figure 5. The ratio is calculated with the flux at $L = 4$ delayed by 2 days to represent the average time required for electrons at $L = 6$ to diffuse to $L = 4$. As can be seen in the bottom plot of Figure 5, the ratio is less than unity for large portions of 1998. During these times, the phase space density gradient is pointing inward and radial diffusion cannot transport electrons to smaller L. If the phase space density at $L = 4$ increases while the ratio is <1, then processes other than radial diffusion must be responsible for the flux enhancement. Examples of this situation can be seen in Figure 5, such as around day 300 indicated by the vertical line. Therefore we find that inward radial diffusion cannot be responsible for all flux enhancements at $L = 4$, consistent with recent phase space density analyses based on Polar measurements [*Selesnick and Blake*, 2000; *O'Brien et al.*, 2003; *Green and Kivelson*, 2004].

[27] The function for the electron lifetime listed in Table 1 for the long-term model run gives a lifetime of 27 days at $L = 4$. Recent evidence of multiple electron decay timescales [*Fennell et al.*, 2005] make it uncertain whether this value of the lifetime is physical. To determine the effect of revising τ, we explore the dependence of the model results on the value of m in the function for the electron lifetime, keeping τ_0 constant. Changing m changes τ for all $L \neq 6$. We find that for $m \gtrsim 4.8$ ($\tau \gtrsim 20$ days at $L = 4$) the results show little change, particularly at $L = 6$. When the L dependence is less steep, the PE at $L = 4$ drops dramatically. For $\tau \approx 15$ days at $L = 4$, the PE_4 falls to 0.44, and to 0.04 when $\tau \approx 10$ days at $L = 4$. This indicates that there is a decay of electrons with a

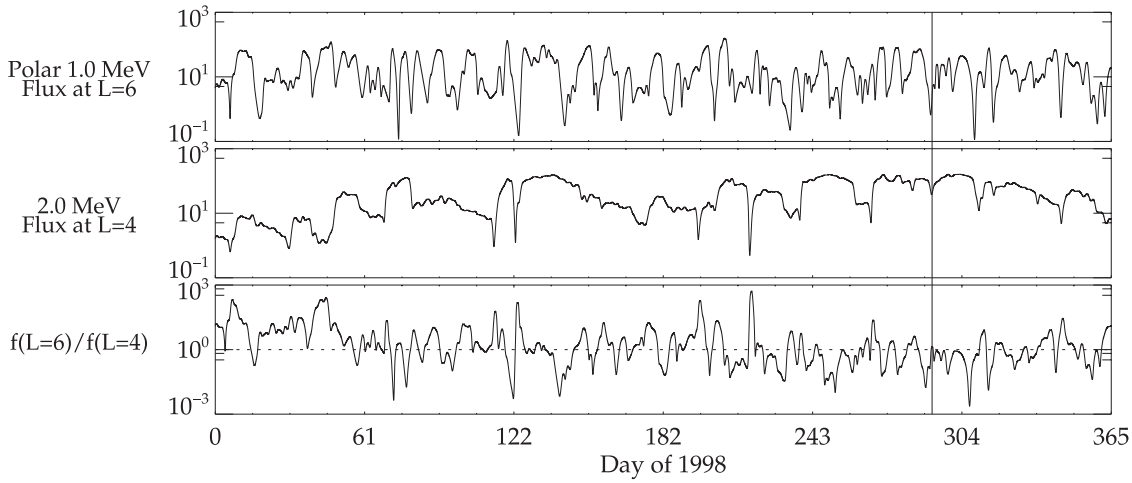

Figure 5. (top) Daily averaged Polar electron flux at L = 6, (middle) daily averaged Polar electron flux at L = 4, and (bottom) ratio of phase space densities at L = 6 and L = 4. The vertical line indicates a time when the phase space density ratio is <1 and there is a flux enhancement at L = 4. See text for further discussion.

lifetime of $\gtrsim$20 days at L = 4 which has a significant effect on the daily averaged electron behavior.

5.2. Short-Term Predictions

[28] We investigate four magnetic storms during 1998 to determine how much the parameter values need to change to predict electron fluxes well during magnetic storms, and how those parameters change from storm to storm. The parameters were tuned for the individual storms to produce the best possible PE_Ts. Ideally, after tuning the model parameters for all of 1998, the same parameter values would produce the best predictions during the magnetic storms. However, the large differences in the final parameter values (see Table 1) demonstrate that this is not the case, and we may need to make some of the parameter values functions of time to account for these differences.

[29] Figure 6 shows measurements of the *Dst* index, IMF B_z, solar wind speed, speed fluctuations, electron flux at geosynchronous orbit and L = 4, and flux predictions during the 2–4 May (above) and 26 June (below) magnetic storms. Figure 7 is the same, but for the 25 September (above) and 19 October (below) storms. As can be seen in Figure 6 and 7, all four storms selected for study have sustained, strongly southward B_z. In addition, the May and September storms were also associated with shocked, high-speed solar wind [*Russell et al.*, 2000; *Moore et al.*, 1999], while the solar wind speed was close to average during the main phases of the other two storms.

[30] The values in Table 1 allow us to discuss the results more quantitatively. With the exception of the May storm, the optimal value of γ_1 is much larger than γ_2 or γ_3, as it is for the long-term prediction. This suggests that solar wind speed is usually the most important driver of electron flux enhancements. For the May storm, $\gamma_1 = \gamma_3 = 0$ gives the best PE, suggesting that the IMF B_z and dynamic pressure have the largest effect on the electron flux during this storm. The PEs of the different storms could be related to the solar wind profiles. For example, the May and September storms are both associated with high solar wind speed, and have the two highest PE_Ts of the four storms. However, the parameter values are not correlated with the solar wind measurements. For the May storm, γ_2 is comparatively much more significant than for the September storm, which corresponds to the lower minimum B_z during the May storm. However, the minimum B_z values for the June and October storms are both $\sim$−15 nT, but γ_2 is a much larger portion of γ_1 for the June storm. The PEs of the June and October storms are quite low, suggesting that it is more likely that other acceleration mechanisms play a larger role in the enhancement of the MeV electrons during these storms, whereas radial diffusion seems to be strongly acting during the May and September storms.

[31] As shown in Table 1, the modeled electron lifetimes also vary significantly over the different time periods. This suggests that the actual electron lifetime changes with magnetic activity and between storms. A variable lifetime can be caused by changes in the effectiveness of a particular loss process or changes in which mechanisms are acting. Losses due to scattering by electromagnetic ion cyclotron waves are more effective at higher plasma densities [*Summers and Thorne*, 2003], while microburst losses due to whistler mode chorus waves are more effective at low plasma densities [*Thorne et al.*, 2005]. Therefore a difference in the plasma densities or location of the plasmapause between storms, or between magnetically active and quiet times, could result in very different total electron lifetimes. However, a portion of the variation in lifetime listed in Table 1 is likely an artifact of our constant source parameters, leading to an incorrect elec-

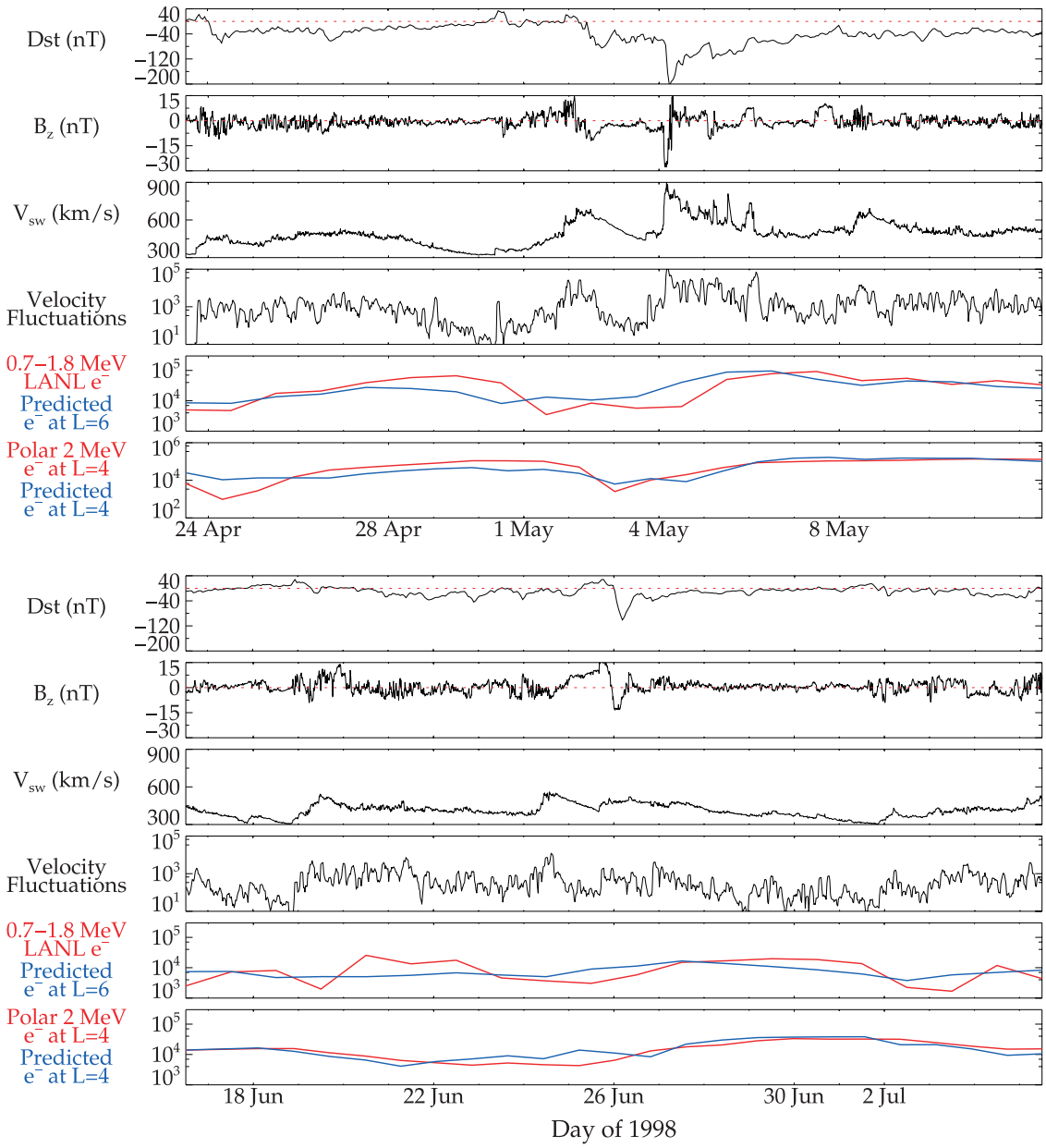

Figure 6. Solar wind measurements and predictions with electron flux measurements at $L = 6$ and $L = 4$ for the (top) 2−4 May 1998 and (bottom) 26 June 1998 magnetic storms.

tron source population. Inaccurate boundary conditions would also affect the values of the diffusion coefficient, indicating that our parameter values may not reflect the relative impact of the different solar wind drivers. This subject will be further addressed using data-based boundary conditions in a future paper.

6. Summary

[32] Radial diffusion is one of several means of accelerating radiation belt electrons to their observed relativistic energies, but is sometimes used alone in models attempting to describe the electron flux variations. To account for the marked enhancements of electron flux during storms, the diffusion coefficient controlling the diffusion rate can be made a function of magnetic activity. Magnetic activity is well correlated with solar wind, which *Li et al.* [2001] used to parameterize their geosynchronous diffusion model. We have extended the Li et al. model to predict the relativistic electron fluxes inside, as well as at, geosynchronous orbit. In this paper, we concentrate on the L shells of 4 and 6. Our model is

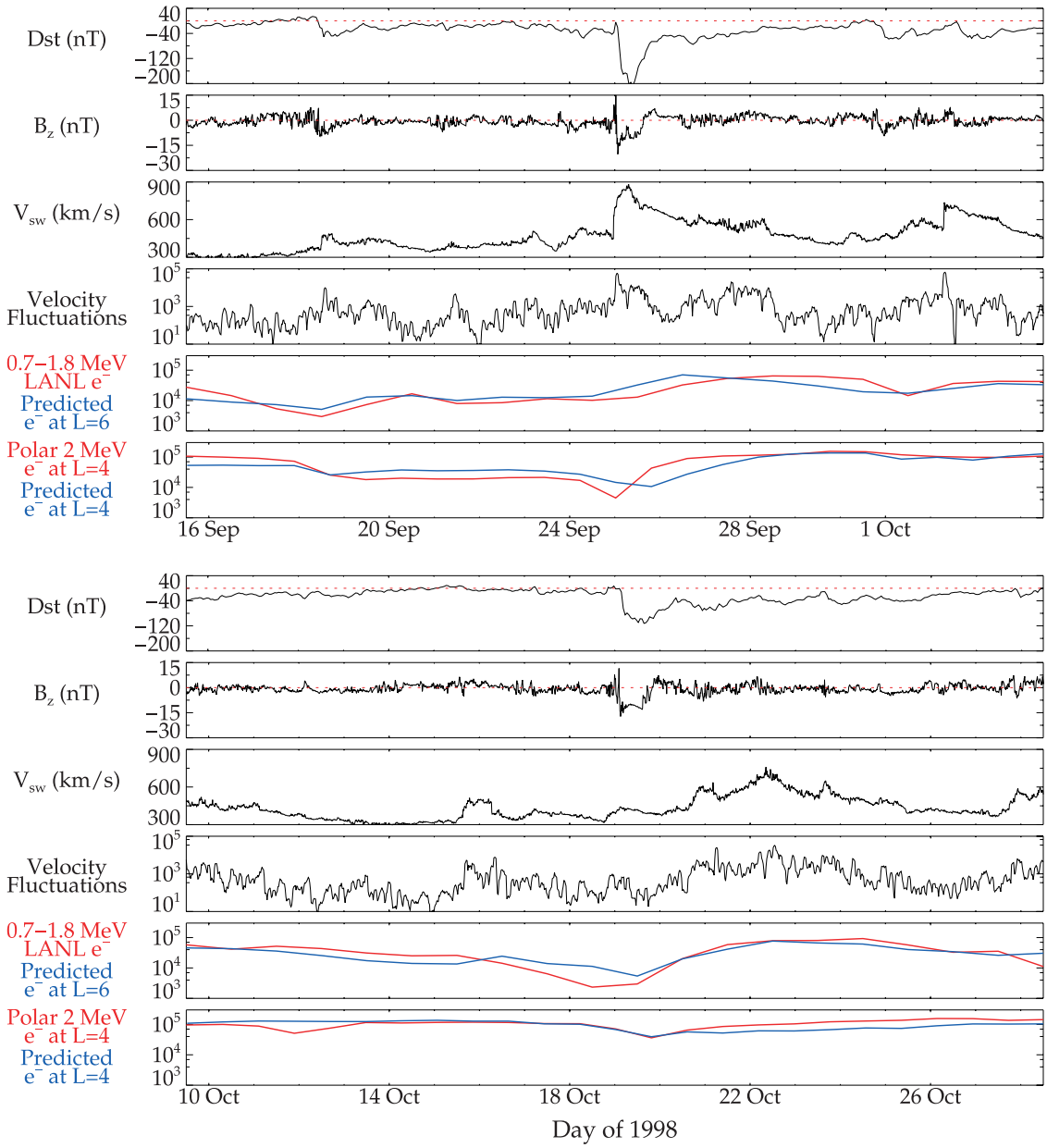

Figure 7. Solar wind measurements and predictions with electron flux measurements at $L = 6$ and $L = 4$ for the (top) September 1998 and (bottom) 19 October 1998 magnetic storms.

able to fairly well reproduce the electron behavior at the two different L shells using the same set of parameters for a 1-year period, suggesting that radial diffusion plays a strong role in energizing the relativistic electrons in the magnetosphere. Since the real-time solar wind data are readily available, this model can be used to provide satellite operators with more than a day of warning of likely enhancement of MeV electrons.

[33] In modeling the storm-time electron fluxes, we found that the diverse nature of magnetic storms requires that we use different parameter values to achieve reasonable predictions. This suggests that our model cannot completely describe the relativistic electron fluxes for all time, and would likely require the inclusion of local heating mechanisms to do so. In addition, the parameter values during storms suggest that the solar wind speed is typically the most important driver of electron flux variations, and that the other solar wind parameters have varying degrees of influence during the different magnetic storms.

[34] **Acknowledgments.** We appreciate the effort by the science teams (WDC for Geomagnetism, Kyoto University, Polar/CEPPAD, LANL energetic particles, Wind/3D, Wind/Mag, ACE/SWEPAM, and ACE/Mag) to make the data available. This work was supported by NASA grants (Polar, NAG5-10474 and NAG5-13518) and NSF grants (CISM, ATM-0233302 and ATM-0101351).

References

Acuna, M. H., et al. (1995), The global geospace science program and its investigations, *Space Sci. Rev.*, *71*, 5.

Albert, J. M. (2002), Nonlinear interaction of outer zone electrons with VLF waves, *Geophys. Res. Lett.*, *29*(8), 1275, doi:10.1029/2001GL013941.

Baker, D. N., et al. (1996), An assessment of spacecraft environmental conditions during the recent Anik E1 spacecraft failure, *ISTP Newsl.*, *6*, 2.

Belian, R. D., G. R. Gisler, T. Cayton, and R. Christensen (1992), High-*Z* energetic particles at geosynchronous orbit during the great solar proton event of October, 1989, *J. Geophys. Res.*, *97*, 16,897.

Blake, J. B., W. A. Kolasinski, R. W. Fillius, and E. G. Mullen (1992), Injection of electrons and protons with energies of tens of MeV into $L < 3$ on March 24, 1991, *Geophys. Res. Lett.*, *19*, 821.

Blake, J. B., et al. (1995), CEPPAD: Comprehensive Energetic Particle and Pitch Angle Distribution experiment on Polar, *Space Sci. Rev.*, *71*, 531.

Brautigam, D. H., and J. M. Albert (2000), Radial diffusion analysis of outer radiation belt electrons during the 9 October 1990 magnetic storm, *J. Geophys. Res.*, *105*, 291.

Elkington, S. R., M. K. Hudson, and A. A. Chan (2003), Resonant acceleration and diffusion of outer zone electrons in an asymmetric geomagnetic field, *J. Geophys. Res.*, *108*(A3), 1116, doi:10.1029/2001JA009202.

Fälthammar, C.-G. (1965), Effects of time-dependent electric fields on geomagnetically trapped radiation, *J. Geophys. Res.*, *70*, 2503.

Fennell, J. F., H. C. Koons, J. L. Roeder, and J. B. Blake (2001), Spacecraft charging: Observations and relationship to satellite anomalies, in *Proceedings of 7th Spacecraft Charging Technology Conference*, Eur. Space Agency Spec. Publ., *ESA SP-476*, p. 279.

Fennell, J. F., J. B. Blake, R. Friedel, and S. Kanekal (2005), The energetic electron response to magnetic storms: HEO satellite observations, in *The Inner Magnetosphere: Physics and Modeling*, *Geophys. Monogr. Ser.*, vol. 155, edited by T. I. Pulkkinen, N. A. Tsyganenko, and R. H. W. Friedel, AGU, Washington, D. C.

Green, J. C., and M. G. Kivelson (2004), Relativistic electrons in the outer radiation belt: Differentiating between acceleration mechanisms, *J. Geophys. Res.*, *109*, A03213, doi:10.1029/2003JA010153.

Gussenhoven, M. S., E. G. Mullen, R. C. Filz, D. H. Brautigam, and F. A. Hanser (1987), New low-altitude dose measurements, *IEEE Trans. Nucl. Sci.*, *34*, 676.

Hilmer, R. V., G. P. Ginet, and T. E. Cayton (2000), Enhancement of equatorial energetic electron fluxes near $L = 4.2$ as a result of high-speed solar wind streams, *J. Geophys. Res.*, *105*, 23,311.

Horne, R. B., and R. M. Thorne (1998), Potential waves for relativistic electron scattering and stochastic acceleration during magnetic storms, *Geophys. Res. Lett.*, *25*, 3011.

Li, X. (2004), Variations of 0.7–6.0 MeV electrons at geosynchronous orbit as a function of solar wind, *Space Weather*, *2*, S03006, doi:10.1029/2003SW000017.

Li, X., I. Roth, M. Temerin, J. R. Wygant, M. K. Hudson, and J. B. Blake (1993), Simulation of the prompt energization and transport of radiation belt particles during the March 24, 1991 SSC, *Geophys. Res. Lett.*, *20*, 2423.

Li, X., et al. (1997), Multisatellite observations of the outer zone electron variation during the November 3–4, 1993, magnetic storm, *J. Geophys. Res.*, *102*, 14,123.

Li, X., M. Temerin, D. N. Baker, G. D. Reeves, and D. Larson (2001), Quantitative prediction of radiation belt electrons at geostationary orbit based on solar wind measurements, *Geophys. Res. Lett.*, *28*, 1887.

Meredith, N. P., R. B. Horne, and R. R. Anderson (2001), Substorm dependence of chorus amplitudes: Implications for the acceleration of electrons relativistic energies, *J. Geophys. Res.*, *106*, 13,165.

Meredith, N. P., R. B. Horne, R. H. Iles, R. M. Thorne, D. Heynderickx, and R. R. Anderson (2002), Outer zone relativistic electron acceleration associated with substorm-enhanced whistler mode chorus, *J. Geophys. Res.*, *107*(A7), 1144, doi:10.1029/2001JA900146.

Moore, T. E., et al. (1999), Ionospheric mass ejection in response to a CME, *Geophys. Res. Lett.*, *26*, 2339.

O'Brien, T. P., K. R. Lorentzen, I. R. Mann, N. P. Meredith, J. B. Blake, J. F. Fennell, M. D. Looper, D. K. Milling, and R. R. Anderson (2003), Energization of relativistic electrons in the presence of ULF power and MeV microbursts: Evidence for dual ULF and VLF acceleration, *J. Geophys. Res.*, *108*(A8), 1329, doi:10.1029/2002JA009784.

Paulikas, G. A., and J. B. Blake (1979), Effects of the solar wind on magnetospheric dynamics: Energetic electrons at the synchronous orbit, in *Quantitative Modeling of Magnetospheric Processes*, *Geophys. Monogr. Ser.*, vol. 21, edited by W. P. Olsen, p. 180, AGU, Washington, D. C.

Roederer, J. G. (1970), *Dynamics of Geomagnetically Trapped Radiation*, Springer, New York.

Rowland, D. E., and J. R. Wygant (1998), Dependence of the large-scale, inner magnetospheric electric field on geomagnetic activity, *J. Geophys. Res.*, *103*, 14,959.

Russell, C. T., et al. (2000), The extreme compression of the magnetosphere on May 4, 1998, as observed by the Polar spacecraft, *Adv. Space Res.*, *25*, 1369.

Selesnick, R. S., and J. B. Blake (2000), On the source location of radiation belt relativistic electrons, *J. Geophys. Res.*, *105*, 2607.

Selesnick, R. S., J. B. Blake, W. A. Kolasinski, and T. A. Fritz (1997), A quiescent state of 3 to 8 MeV radiation belt electrons, *Geophys. Res. Lett.*, *24*, 1343.

Schulz, M., and L. Lanzerotti (1974), *Particle Diffusion in the Radiation Belts*, Springer, New York.

Stone, E. C., A. M. Frandsen, R. A. Mewaldt, E. R. Christian, D. Margolies, J. F. Ormes, and F. Snow (1998), The Advanced Composition Explorer, *Space Sci. Rev.*, *86*, 1.

Summers, D., and R. M. Thorne (2003), Relativistic electron pitch-angle scattering by electromagnetic ion cyclotron waves during geomagnetic storms, *J. Geophys. Res.*, *108*(A4), 1143, doi:10.1029/2002JA009489.

Summers, D., R. M. Thorne, and F. Xiao (1998), Relativistic theory of wave-particle resonant diffusion with application to electron acceleration in the magnetosphere, *J. Geophys. Res.*, *103*, 20,487.

Temerin, M., I. Roth, M. K. Hudson, and J. R. Wygant (1994), New paradigm for the transport and energization of radiation belt particles, *Eos Trans. AGU*, *75*(44), Fall Meet. Suppl., 538.

Thorne, R. M., T. P. O'Brien, Y. Y. Shprits, D. Summers, and R. B. Horne (2005), Timescale for MeV electron microburst loss during geomagnetic storms, *J. Geophys. Res.*, *110*, A09202, doi:10.1029/2004JA010882.

Vennerstrom, S. (1999), Dayside magnetic ULF power at high latitudes: A possible long-term proxy for the solar wind velocity, *J. Geophys. Res.*, *104*, 10,145.

X. Li, Laboratory for Atmospheric and Space Physics, University of Colorado, 1234 Innovation Dr., Boulder, CO 80303, USA. (lix@paracel.colorado.edu)

R. S. Selesnick, The Aerospace Corporation, Los Angeles, CA 90009, USA.